

# USING SPECTRAL AND SPATIAL INFORMATION COUPLED WITH MATHEMATICAL MORPHOLOGY FOR OIL SPILL DETECTION IN MULTISPECTRAL IMAGERY

**Ling-Ling Tsao**

Graduate Student/Graduate Institute of  
Space Science, National Central University,  
Chungli, Taiwan  
E-mail: llt00529@gmail.com

**Hong-Ming Kao**

PhD Student/Institute of Applied  
Geosciences, National Taiwan Ocean  
University, Keelung, Taiwan  
E-mail: hartge1020@yahoo.com.tw

**Hsuan Ren**

Associate Professor/Center for Space and  
Remote Sensing Research, National Central  
University, Chungli, Taiwan  
E-mail: hren@csrsl.ncu.edu.tw

**KEY WORDS:** oil spill detection, anomaly detection, RX detector, spatial feature images.

## ABSTRACT

How to detect, monitor and track the oil spill on the sea surface are always very important tasks, since it is harmful to the ecological environment. The remotely sensed image provides an effective and efficient way to monitor the sea area. This study focuses on the detection of oil slick on sea surface using multispectral imagery technology. Since the oil spill usually only occupies a few pixels compare to the sea area in the image scene, it can be considered as an anomaly. The widely used RX algorithm, designed for anomaly detection, did not produce satisfied results. Although it successfully detects the oil slick, but the light reflections from the small waves are also detected as false alarm. In order to discriminate oil slick from the other interferers, spatial features are introduced into anomaly detection. The spatial features of oil slick are very different from that of the small wave reflection. The former often forms a connected area, but the latter ones usually separated and spread in the image. Our proposed method is to extract different spatial features form the images and combine with spectral information, and then perform anomaly detection with both spectral and spatial features to improve the oil spill detection. In the experiment, we adopt SPOT multispectral images for performance analysis.

## 1. INTRODUCTION

Taiwan plays a key role in southeastern Asia's transportation. Nowadays, marine transit is still an important way for import and export. The oil spill on the sea surface caused by human activities occurs from time to time and is harmful to the marine environment. Using the remotely sensed images to detect this unwelcomed hazard material on the sea surface is a convenient and effective approach.

Target detection can be implemented in two aspects. One is using target's unique character of spectral reflection; the other is using the spatial textural distribution to discriminate them from the background. Because the spectral information between oil slick and the surrounding sea water were very different, and it usually only occupied a few pixels, the famous RX algorithm [1], [2] is first applied to detect the oil slick as an anomaly. Although it successful detects oil slick, but the result also shows other interferers produced by marine phenomenon. In order to reduce the influence of the interference, we introduce the Spatial Feature Information [3], [5] and employ the spatial textures to separate oil slick from the background. After adopted Spatial Feature Information algorithm, differences between oil slick and background can be easily revealed. After spatial feature extraction steps, we implement RX algorithm on both spectral and spatial features and the oil slick area can get higher separation from the background. Finally, a threshold operation is applied to locate the oil slick.

## 2. ANOMALY DETECTION

The oil spill on the sea surface usually covers a small area in image. In our study, we view oil slick as an anomaly, and the rest as background. The famous RX algorithm for anomaly detection is discussed.

### 2.1 RX detector

The RX algorithm was development by Reed and Yu (1990). It can detect anomalies without any priori information of target or background, and it operates under two assumptions: the target only occupies a few pixels in image and its spectrum is very different from the background [1], [2], [4]. It can be expressed as following.

$$\delta_{RXD}(\mathbf{r}) = (\mathbf{r} - \mu)^T \mathbf{K}_{L \times L}^{-1} (\mathbf{r} - \mu) \quad (1)$$

where  $\mathbf{r}$  is the vector of pixel,  $L$  is the number of spectral bands,  $\mu$  is the global sample mean vector and  $\mathbf{K}_{L \times L}$  is the sample covariance matrix of the image. Since some pixels have very different spectrum from others, they give higher score with Eq. (1) on image, and then the anomaly pixels can be found.

## 3. SPATIAL FEATURE INFORMATION

Spatial Feature Information calculates the relationship between one pixel's gray level and its surrounding eight pixels' in the image. Spatial features could catch the texture, boundary and shape information. In this study, we used two kinds of Spatial Feature Information in [3], [5]: Gray Level Histogram and Texture Feature Coding Method.

### 3.1 Gray Level Histogram

Gray Level Histogram was extracted from the distribution of pixel's brightness in the image. We first count the number of pixels with the same gray value for each gray level, and then calculate the three features according to the statistic property; mean  $\mu = \sum_{k=0}^{255} k \cdot p(k)$ , variance

$$\sigma^2 = \sum_{k=0}^{255} (k - \mu)^2 \cdot p(k) \quad \text{and Kurtosis} \quad \mu_4 = \frac{1}{4\sigma^4} \sum_{k=0}^{255} (k - \mu)^4 \cdot p(k) - 3.$$

Where  $k$  is gray level, and  $p(k)$  is the probability of gray level  $k$ , i.e., the number of pixels with gray value  $k$  divide by the total number of pixels in the image.

### 3.2 Texture Feature Coding Method

Texture Feature Coding Method computes the relation of central pixel's four directions variation in the mask. The four directions are first connection: horizontal direction ( $0^\circ$ - $180^\circ$ ) and vertical direction ( $90^\circ$ - $270^\circ$ ) which shows in Fig. 2; Second connection: the upper right to lower left ( $45^\circ$ - $225^\circ$ ) and the upper left to lower right ( $135^\circ$ - $315^\circ$ ) which shows in Fig. 3. In order to code pixels in image, it takes a  $3 \times 3$  mask on pixel in image and gives those nine pixels a serial number which shows in Fig. 1.

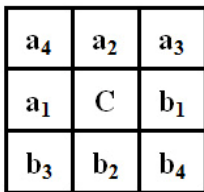


Fig. 1

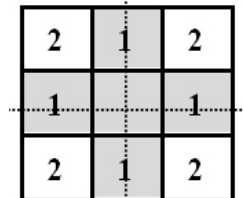


Fig. 2

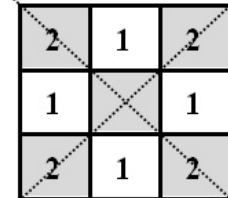
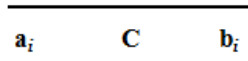


Fig. 3

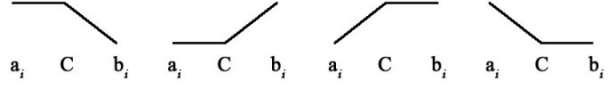
Fig. 1 shows Texture Spectrum serial number. Fig. 2 Shows Texture Feature Coding Method serial number. Fig. 3 Shows first connection. Fig. 4 Shows second connection.

Where  $C$  is the central pixel and its surrounding eight pixels are marked as  $\{a_1, a_2, a_3, a_4, b_1, b_2, b_3, b_4\}$ . Selected three pixels on four directions variously and calculated odds of two neighbor pixels. According to the variation of three pixels on same direction we could code pixels in image. There are four possible situations with three connected pixels in one direction:

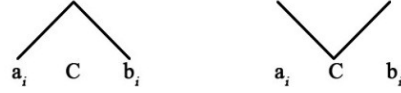
I.  $(|a_i - C| \leq \Delta) \cap (|C - b_i| \leq \Delta)$



II.  $(|a_i - C| \leq \Delta) \cap (|C - b_i| > \Delta) \cup [(|a_i - C| > \Delta) \cap (|C - b_i| \leq \Delta)]$



III.  $[(a_i - C > \Delta) \cap (C - b_i > \Delta)] \cup [(C - a_i > \Delta) \cap (b_i - C > \Delta)]$  IV.  $[(a_i - C > \Delta) \cap (b_i - C > \Delta)] \cup [(C - a_i > \Delta) \cap (C - b_i > \Delta)]$



Where the  $\Delta$  is the tolerance error, and there are two ways to assign this parameter: one is fixed relation with  $\Delta$  between 1 and 3; another way is Just Noticeable Difference (JND) which showed in Eq. (2),  $\alpha$  and  $\beta$  are parameters for JND, the optimized value are 17 and  $3/128$ .  $bg$  is the average value of eight neighborhood pixels. And  $s$  is the weight of tolerance error.

$$\Delta = s \times \begin{cases} \alpha [1 - (\frac{bg}{127})^{1/2}] + 3 & \text{if } bg \leq 127 \\ \beta (bg - 127) + 3 & \text{if } bg > 128 \end{cases} \quad (2)$$

According to table 1, the classified number is given by combining the direction of the first and second connection.

Table 1 Texture feature coding method classification

		First connection				
		Categories	I	II	III	IV
Second connection	I	1	2	3	4	
	II	2	5	6	7	
	III	3	6	8	9	
	IV	4	7	9	10	

Define  $\kappa$  as the classified result of combining horizontal direction and the upper right to lower left direction,  $\lambda$  as the classified result of combining vertical direction and the upper left and lower right direction. Every pixel has its  $\kappa$  and  $\lambda$ , and the texture feature number (TFN) is the multiplication of  $\kappa$  and  $\lambda$  as shown in Eq. (3).

$$TFN(x, y) = \kappa(x, y) \times \lambda(x, y) \quad (3)$$

TFN has 42 possible numbers between 1 and 100, and it is rearranged into 0 to 41. If the number is large, then the pixel's gray value is difference from its neighbor, on the other hand, if the pixel has similar gray value to its surroundings, the number will be small. There are three indexes calculated from TFN as following:

**3.3.1 Coarseness:** Shows in Eq. (4), Coarseness counts the frequency of the largest TFN. For the largest number of TFN, the pixel is classified as situation IV in all four directions.

$$Coarseness = \sum_{\Delta=0}^{\Delta^*} P_{\Delta}(41), \quad P_{\Delta}(n) = \frac{N_{\Delta}(n)}{N}, n \in \{0,1,2,\dots,41\} \quad (4)$$

Where  $P_{\Delta}$  is histogram of TFN,  $N_{\Delta}$  is TFN occurring times and  $N$  is the number of occurring times for all TFN.

**3.3.2 Homogeneity:** Just like the concept of coarseness, Homogeneity counted the smallest variation's occurring frequency in TFN. The number of TFN is zero.

$$Homogeneity = \sum_{\Delta=0}^{\Delta^*} P_{\Delta}(0) \quad (5)$$

**3.3.3 Mean Convergence (MC):** It can evaluate the level between TFN and average.

$$MC = \sum_{n=0}^{41} \frac{|n \cdot P_{\Delta^*}(n) - \mu_{\Delta^*}|}{\sigma_{\Delta^*}} \quad (6)$$

Where  $\mu_{\Delta^*}$  is TFN's average when tolerance error equal to  $\Delta^*$ ,  $\sigma_{\Delta^*}$  is TFN's standard deviation when tolerance error equal to  $\Delta^*$ .

**3.3.4 Variance:** Variance indicates the variation between number of TFN and its mean. If the variation is larger variance would be greater.

$$Variance = \sum_{n=0}^{41} (n - \mu_{\Delta^*})^2 \cdot P_{\Delta^*}(n) \quad (10)$$

## 4. EXPERIMENTS

In this section, we adopt 3-band SPOT1 multispectral images for the experiments. On Jan. 14, 2001, the Amorgos was grounded on the sea shore of Long-Luan Pool, Kenting. Under the gale and wave, the cargo ship was broken and the oil is spilled on the sea. As shown in Fig. 4(a), SPOT1 captured the whole scene of coast of Kenting of the image size is 200×200 pixels. The oil slick is distributed from northeast to southwest.

According to sea surface has weak inflection in near IR band [6], and oil slick is usually dark in image, we select a threshold value from band3 to separate ground and ocean, and expand three bands' gray values of Fig. 4(a) into 0 to 255, the results show in Fig. 4(b)-(d).

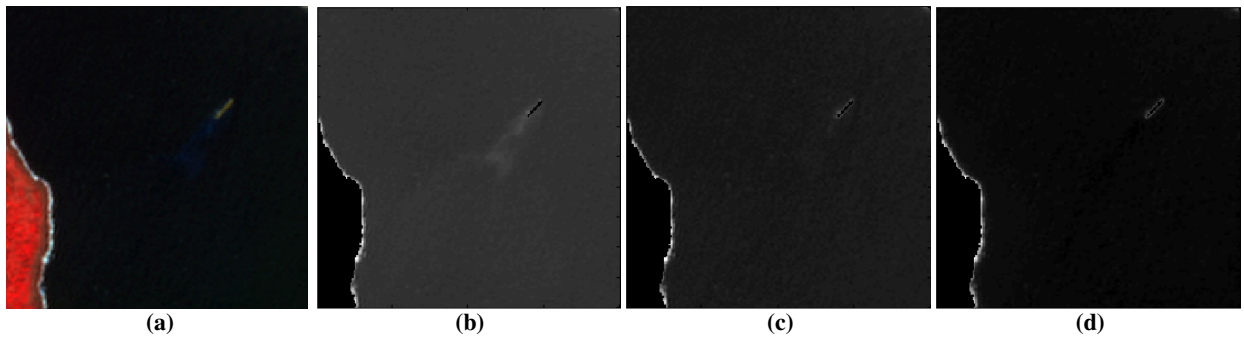
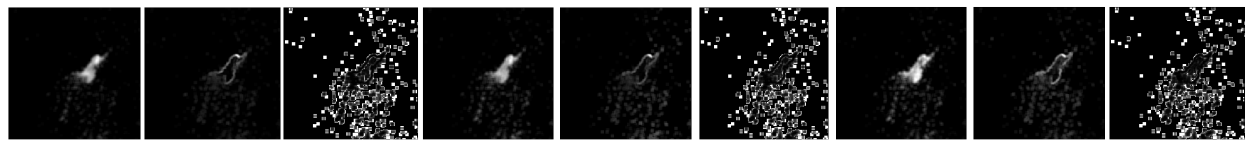
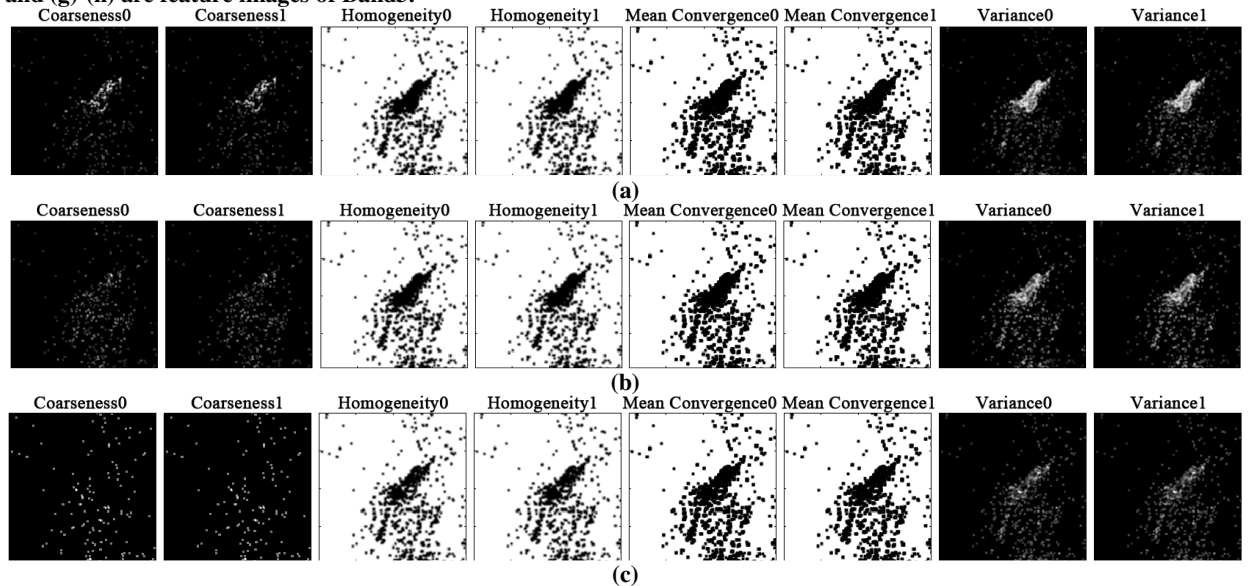


Fig. 4 (a) SPOT1 image scene of Kenting coast. (b)(c) and (d) are the images of (a)'s band1, band2 and band3 which have expanded gray values into 0 to 255.

We implement Spatial Feature Information which is mentioned in part 3 to calculate feature images of each band. There are two kinds feature images: Gray Level Histogram and Texture Feature Coding Method. Those feature images show in Figs. 5-6. We choose 12 feature images of three bands from total 33 images. Those feature images are Mean and Variance of three bands, Coarseness of band1, and Variance of band1 and band2. From those feature images, we can be aware there are many pixels spread on the sea surface which are induced by marine phenomena. In order to reduce that interference, we adopt the “open-close” algorithm of mathematical morphology to clear tiny noise from sea surface phenomena. After implement “open-close” algorithm, we identify the 12 feature images as a new image cube.



(a) Mean (b) Variance (c) Kurtosis (d) Mean (e) Variance (f) Kurtosis (g) Mean (h) Variance (i) Kurtosis  
**Fig. 5 Feature images of Gray Level Histogram. (a)-(c) are feature images of Band1, (d)-(f) are feature images of Band2 and (g)-(h) are feature images of Band3.**



**Fig. 6 Feature images of Texture Spectrum. 0 stands for fixed relation and 1 stands for JND. (a) is feature image of Band1, (b) is feature image of Band2 and (c) is feature image of Band3.**

Fig. 7 shows the RX result on new image cube according to Eq. (1). In this figure, oil slick gives higher score. After applying a threshold to the RX result, as shown in Fig.8, the oil slick is clearly viewed but with some white pixels as interferers. We implement “open-close” again to clear tiny interference and circle the area on the original image, the results are shown in Fig 9 and Fig 10 respectively. Same procedure is applied to the original image cube, as shown in Figs. 11 to 14. Comparing the result for original image with the result for new image cube, new image cube can detect the oil slick with better performance.

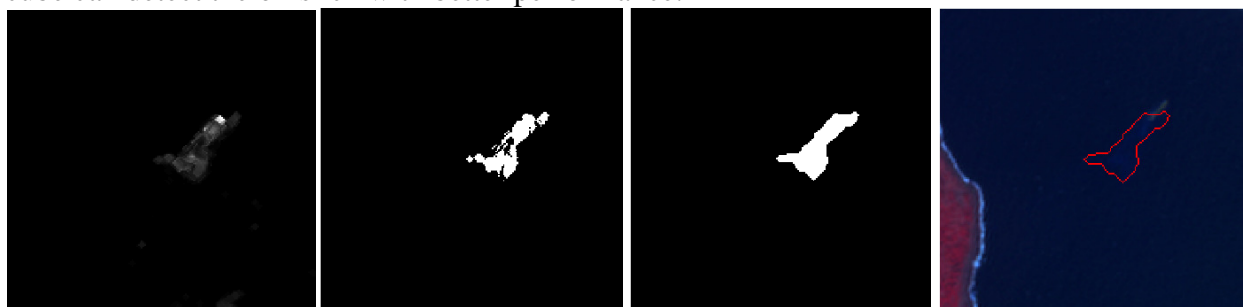


**Fig. 7 RX result for new cube**

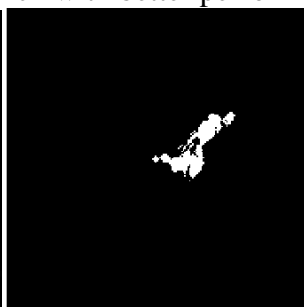


**Fig. 8 Thresholded image**



**Fig. 9 Detected Area**

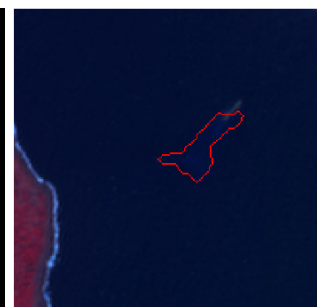


**Fig. 10 Area on SPOT1 image**

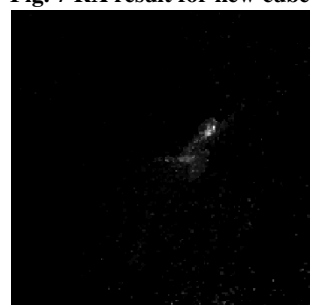


**Fig. 11 RX result**

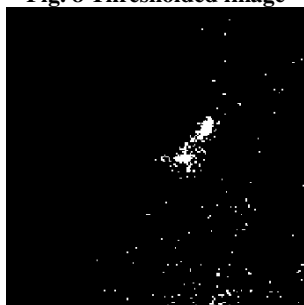


**Fig. 12 Thresholded image**



**Fig. 13 Detected Area**

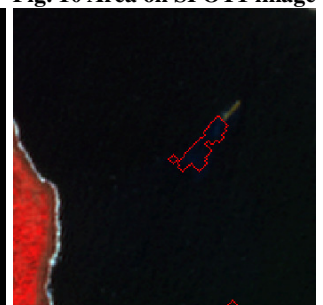


**Fig. 14 Area on SPOT1 image**

## 5. CONCLUSIONS

From the experimental results, we use the Spatial Feature Information to discriminate oil slick and interference which induced by marine phenomena. And adopt “open-close” algorithm of mathematical morphology to reduce the interference in feature images. The RX algorithm is applied; it can detect the oil spill on sea surface, but still reveals some interference produced by marine phenomena. In order to remove those remaining interference we take “open-close” algorithm again. In this study, we introduce Spatial Feature Information to improve the result of RX algorithm. Finally, we apply mathematical morphology to the image; it further filters out the interference of the sea phenomena. Therefore, our method improves the original RX algorithm in oil slick detection.

## 6. REFERENCES

- [1] Reed, I. and Yu X., 1990. Adaptive Multiple-Band CFAR Detection of an Optical Pattern with Unknown Spectral Distribution. *IEEE transactions on acoustics, speech, and signal processing*, Vol. 38, No. 4, pp. 1760-1770.
- [2] C.-I Chang and S.-S Chiang, Anomaly Detection and Classification for Hyperspectral Imagery, *IEEE transactions on geoscience and remote sensing*, vol.40, no.6, pp. 1314-1325, 2002.
- [3] Huang Jun-zhong. The Mass Detection in Mammography Using Feature Images. Master Dissertation, National Central University, 2006.
- [4] Chen Hsien-Ting. Anomaly Detection for Hyperspectral Imagery. Master Dissertation, National Central University, 2006.
- [5] Liao Yu-China, The Mass Detection in Mammography Using Texture Analysis. Master Dissertation, National Cheng Kung University. 2002.
- [6] Taylor, S, 1992. 0.45 to 1.1  $\mu\text{m}$  Spectra of Prudhoe Crude Oil and of Beach Materials in Prince William Sound, Alaska, CRREL Special Report No. 92-5, Cold Regions Research and Engineering Laboratory, Hanover, New Hampshire, 14 p.